

Process Monitoring of Turning and Model Adaptation for Smart Machining Systems

J. C. Heigel, R. W. Ivester

National Institute of Standards and Technology, Gaithersburg, MD 20899, USA

Abstract

Cutting force models, often developed from a narrow set of empirical data, provide insight into the physical properties of cutting, but the extreme physical phenomena of metal cutting and the many uncertainties in an industrial setting (machine tool, workpiece material, tooling, environmental conditions) hinder predictability. In order to improve the practicality of model-based decision making in an industrial machining environment, this paper introduces a method to adapt parameters of a traditional empirical model in response to on-line measures of process performance. This method enables Smart Machining Systems to self-monitor production performance and adapt models and process parameters to the conditions encountered in production environments, reducing the need for expensive empirical tests.

Keywords: Smart Machining Systems, In-Process Monitoring, Adaptive Modeling, Uncertainty

1. Introduction

In 1998, Merchant estimated that 15 % of the value of all mechanical components manufactured worldwide is derived from machining operations [1]. Despite the economic and technical importance of machining, the cost of research limits industrial capability to improve machining efficiency. Large empirical databases and guidelines [2][3][4] aid in process design, but their relevance diminishes with the introduction of new tool materials, machines, and workpiece materials.

Recent, dramatic improvements in the capabilities of high-speed machining centers have enabled speeds and feed rates to increase by an order of magnitude, rendering previously established databases and handbook tables essentially useless. Smart Machining Systems (SMS) provide a means for industry to keep pace with changing production capabilities while avoiding costly experimentation. The SMS research program at the National Institute of Standards and Technology (NIST) defines a Smart Machining System as having the following characteristics: 1) self-knowledge and communication of its capabilities to other parts of the manufacturing enterprise, 2) self-monitoring and optimization of its operations, 3) self-assessment of the quality of its work, and 4) self-learning and performance improvement over time [5][6][7].

Smart Machining Systems use predictive models

and associated uncertainties to provide robust predictions of forces and other criteria that approach, but do not exceed, process limitations in order to improve manufacturing efficiency. However, the extreme physical phenomena inherent in machining systems and the many uncertainties in industrial environments render the realization and application of predictive machining models difficult. The extremely complex plastic flow of the workpiece material into the expended chip makes prediction difficult even with sophisticated finite element modeling (FEM) software [8, 9]. Basic flow stress data on material behavior under such complex conditions is unavailable for most materials [10][11]. Therefore, FEM software relies on empirical application dependant data to model fundamental material behavior. Additionally, the variability in tooling, workpiece material, machine tools, and environmental conditions in production applications significantly increases the uncertainty of the most accurate models. This has limited the industrial application of machining models, particularly for small corporations or small job sizes which impose practical limitations on experimentation.

This paper presents a method for machine tools to monitor cutting performance during production operations to reduce reliance on testing. Dynamometer tests provide a model between the

Spindle Load Voltage (SLV) signal, available in most controllers, and the measured cutting force. The model of the relationship between spindle load and cutting force provides a means to monitor cutting performance during part production. The resulting cutting performance information enables adaptation of cutting force model parameters to account for differences between the experimental and production environment.

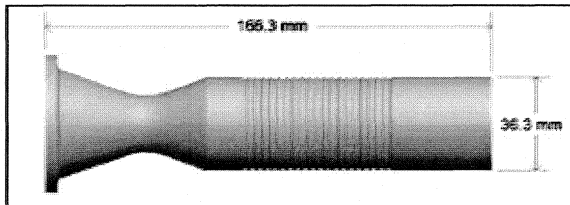


Figure 1: Test Part

Non-intrusive methods for production environment data collection increase understanding of operations and provide a competitive advantage. Furthermore, production data enlarges the modeling dataset to account for more process variations than traditional experiments.

2. Experimental Method

This paper presents results for turning American Iron and Steel Institute (AISI) 1045 steel cold-rolled stock on a 22 kW lathe. Experimental tests performed on 127 mm and 51 mm diameter stock included steady-state cuts with a variety of inserts to develop cutting force models and the relationship between spindle load and cutting force. Analog low-pass filtering at 50 Hz of 3-axis dynamometer force measurements and machine controller SLV before conversion to digital signals prevented aliasing effects. Production of test parts (Figure 1) from 51 mm diameter stock involved the same methodology for monitoring SLV as in the experimental test; however, part production included use of coolant while experimental tests did not.

For production of the test part, we selected a CNMG432-RN 80° coated carbide insert to rough cut the outer diameter (OD) and the face, and a VCMR331 35° coated carbide insert to rough cut the complex features and finish the OD.

3. Cutting Force Empirical Model

Creation of dimensionless cutting force model power-law relationships as a function of depth (d), feed (f), and surface speed (v) (Equation 1) requires converting (d), (f), and (v) to their respective dimensionless forms d , f , and v , through division by their unity dimensions, $d_o=1$ mm, $f_o=1$ mm/rev, and $v_o=1$ m/min (Equation 2). Conversely, converting the dimensionless predicted cutting force F_P into predicted cutting

force F_P' , requires multiplication by the unity dimensioned $F_{Po}=1$ N (Equation 3).

$$F_P = K * d^a * f^b * v^c \quad (1)$$

$$d = d'/d_o \quad f = f'/f_o \quad v = v'/v_o \quad (2)$$

$$F_P' = F_P * F_{Po} \quad (3)$$

An iterative approach to single variate regression analysis of the relationships between dimensionless forces F_P and process parameters v , f , and d requires the introduction of three dimensionless intermediate correlation parameters C_d , C_f , and C_v (Equation 4).

Calculation of the coefficient K relies on assumed initial conditions of $a = 1$, $b = 1$, $c = 1$. Repeated regression on C_d , C_f , and C_v led to converged values at $K = 2156$, $a = 0.906$, $b = 0.787$, and $c = -0.040$ (Figure 2). Note that the vertical scales in Figure 2 are different for plots A, B, and C.

$$C_d = \frac{F_i}{f^b * v^c} \quad C_f = \frac{F_i}{d^a * v^c} \quad C_v = \frac{F_i}{d^a * f^b} \quad (4)$$

Equation 5 provides an estimate for the expanded uncertainty ΔF_P describing the variability of the data with a coverage factor of 2, using data set size ($N = 143$) and dimensionless cutting force for an individual test (F_i) [12].

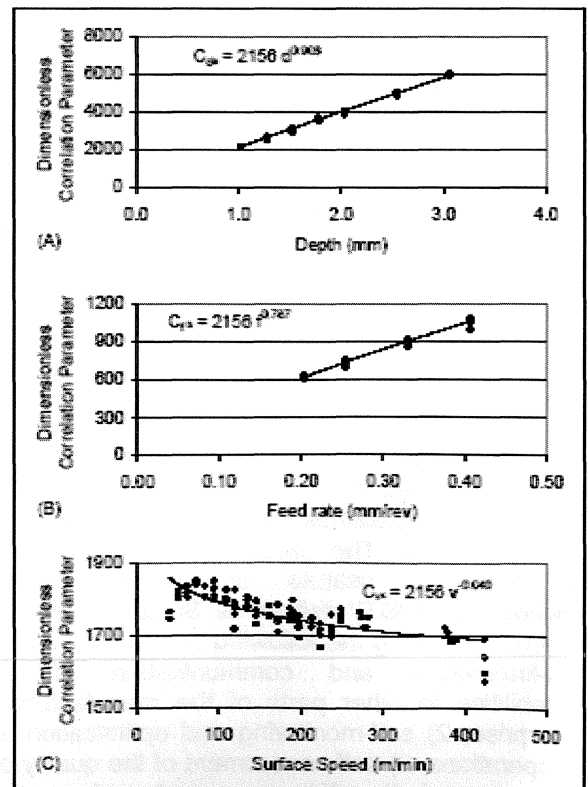


Figure 2: CNMG-432RN Model Plots for Depth (A), Feed (B), and Speed (C)

Equation 6 presents the model of cutting force for the CNMG-432RN insert as a function of depth, feed, and speed resulting from the iterative regression analysis.

$$\Delta F_p = 2 * \sqrt{\frac{\sum_{i=1}^N (F_p - F_i)^2}{N-4}} \tag{5}$$

$$F_p = 2156 * d^{0.936} * f^{0.787} * v^{-0.040} \tag{6}$$

4. Smart Machine Self-Monitoring

The data from the experimental tests establishes a relationship between SLV and cutting force. By subtracting the average SLV before tool engagement from the average steady-state SLV after tool engagement, we obtained the net spindle load as the portion of the SLV attributable to cutting force. Figure 3 shows the relationship between measured dynamometer force (F), average net SLV (L), and diameter (D) which has been measured after each test. The least-squares method yielded four zero-intercept linear relationships (Equation 7), where m is the linear fit slope.

$$F = \frac{m * L}{D} \tag{7}$$

Equation 8 provides an estimate for the expanded uncertainty describing the variation in observed m values for each experiment ($\Delta m, \pm 2\sigma$) using the spindle speed data set size (n) and the linear slope of an individual data point (M_i). Equation 9 calculates M_i using measured force (F_i), diameter (D_i), and SLV (L_i). Table 1 shows m and Δm for each spindle speed (ϕ).

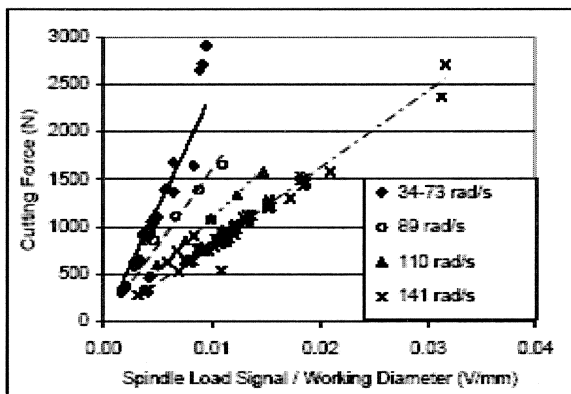


Figure 3: Comparison of Force, SLV, and Diameter

$$\Delta m = 2 * \sqrt{\frac{\sum_{i=1}^n (M_i - m)^2}{n-1}} \tag{8}$$

ϕ (rad/s)	(rpm)	m (N mm/V)	Δm (N mm/V)	n
34.0	325	2.40E+05	9.2E+04	27
57.6	550	2.40E+05	4.8E+04	5
69.4	663	2.40E+05	1.2E+04	4
73.3	700	2.40E+05	3.3E+04	6
89.0	850	1.60E+05	5.7E+04	5
110.0	1050	1.09E+05	1.2E+04	5
141.4	1350	8.10E+04	1.4E+04	91

Table 1: Spindle Speed, m , Δm , and data set size

$$M_i = \frac{F_i * D_i}{L_i} \tag{9}$$

Figure 4 presents the relationship used to calculate the predicted m value (m_p) for the range of spindle speeds from Table 1. The modeled data indicates two trends with a transition point at a spindle speed of 70.2 rad/s (670 rpm). The predicted slope m_p conforms to a constant value below the transition point (Equation 10). The predicted slope follows a power law trend above the transition point (Equation 11). The aggregate of the Δm values produces the predicted m value uncertainty (Δm_p).

$$m_{p \phi \leq 70.2 \text{ rad/s}} = 2.40 * 10^5 \tag{10}$$

$$m_{p \phi > 70.2 \text{ rad/s}} = 1.18 * 10^{10} * \phi^{-1.66} \tag{11}$$

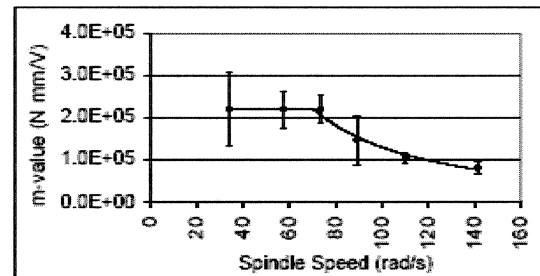


Figure 4: Relationship of m and Spindle Speed

Equation 12 determines the calculated force (F_c) from the SLV signal. Equation 13 quantifies the propagation of uncertainty for calculating cutting force uncertainty (ΔF_c) with a coverage factor of 2 based on the uncertainties associated with the model parameters m_p , L , and D . SLV noise (ΔL), along with part deflection and machine error which affect the diameter uncertainty (ΔD) affect the calculation of cutting force during part production.

$$F_c = \frac{m_p * L}{D} \tag{12}$$

$$\Delta F_c = F_c * \sqrt{\left(\frac{\Delta m_p}{m_p}\right)^2 + \left(\frac{\Delta L}{L}\right)^2 + \left(\frac{\Delta D}{D}\right)^2} \tag{13}$$

5. Cutting Process Monitoring

Since the spindle damping characteristics, workpiece inertia, sampling frequency, and controller response time significantly affect the SLV process signal, we consider only steady-state cutting during the production of the test part. The spindle load required to maintain desired spindle speeds varies during part production due to changes in spindle speed, decreasing workpiece inertia from the material loss, and changes in spindle efficiency as a result of temperature and load fluctuations. Figure 5 shows the raw SLV signal obtained during the test part production. Subtracting the average SLV signal before the engagement of a cut from the steady-state SLV signal during a cut determined the net SLV value attributable to the cutting force. Load spikes attributable to spindle speed changes and cut engagements and disengagements have been removed from Figure 5a for clarity and have been retained in Figure 5b to properly illustrate signal analysis concerns.

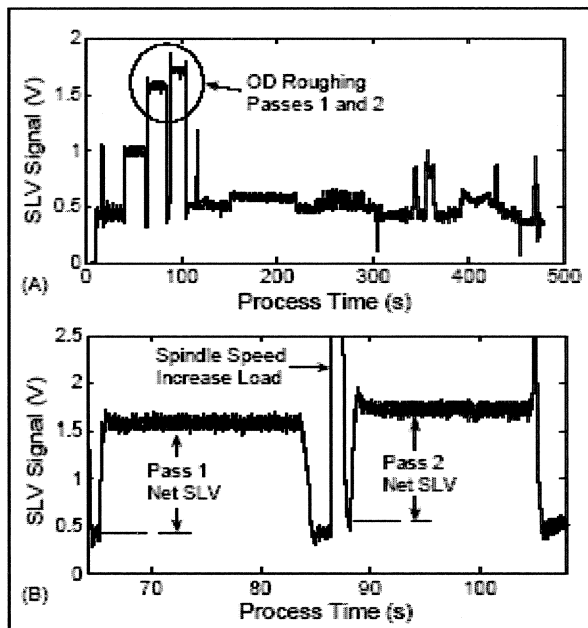


Figure 5: Gross SLV Production Signal of Test Part for Entire Process (A), and OD Roughing (B)

Pass	Process Parameters			Forces	
	d (mm)	f (mm/rev)	v (m/min)	Predicted (N)	SLV Calculated (N)
1	2.94	0.318	1507	1875 ± 77	1605 ± 334
2	2.96	0.318	1754	1889 ± 77	1491 ± 313

Table 2: CNMG-432RN Production OD Roughing Passes

Interpretation of the numerical control instructions for part production provides values for the instantaneous cutting diameter and spindle speed to convert the net SLV to cutting force. Figure 6

compares the SLV calculated cutting force and uncertainty bands with Equation 12 and Equation 13 and the modeled cutting force and uncertainty bands from Equation 5 and Equation 6.

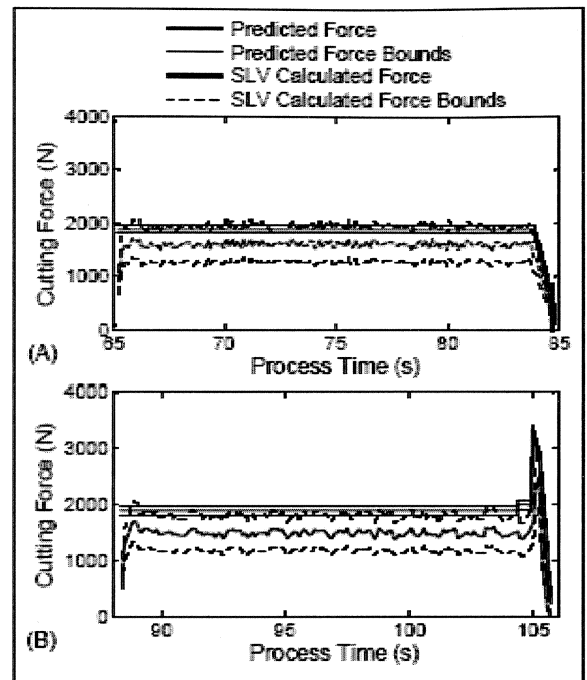


Figure 6: Comparison of SLV Calculated Force to Model Predicted Force: OD Roughing Pass 1 (A) and Pass 2 (B)

Using the same process produces similar results for the other OD roughing pass. Table 2 shows the process parameters, predicted cutting forces, and steady state calculated cutting forces for these passes.

6. Smart Machine Learning

When a machine tool is able to monitor its operations, it can record data for use by an operator or use the data to adapt to changing conditions. More specifically, the machine can use the steady-state cutting force data to improve upon optimization models by increasing the size of the model creation datasets. It is beneficial to incorporate the production force data into the model construction dataset for three reasons: 1) to identify or account for uncontrolled changes in the process due to factors such as material inhomogeneity (as illustrated by the hardness profile given in Figure 7), 2) to expand the model application range, and 3) to improve the model trend accuracy through an increasing dataset. The average calculated cutting forces from Table 2 have been added to the model dataset (Figure 8). Adjusting the power fit to the new dataset results in the new cutting force model in Equation 14.

$$F_p = 2286 * d^{0.819} * f^{0.755} * v^{-0.055} \tag{14}$$

7. Summary

The methodology discussed in this paper equipped a turning center with the necessary tools to monitor process cutting forces. The acquired force data enables the machine to adapt force models to account for changes in workpiece material and other uncontrolled process parameters, thus reducing the need for application specific empirical testing while improving machining efficiency without increasing cost.

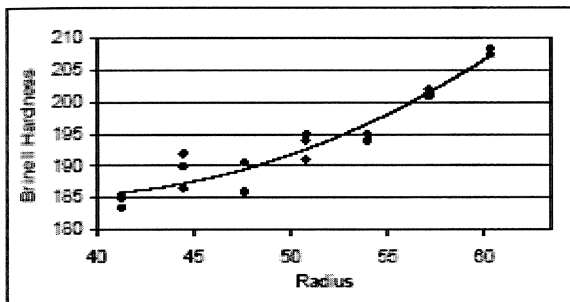


Figure 7: Hardness Profile for 127 mm Diameter Stock

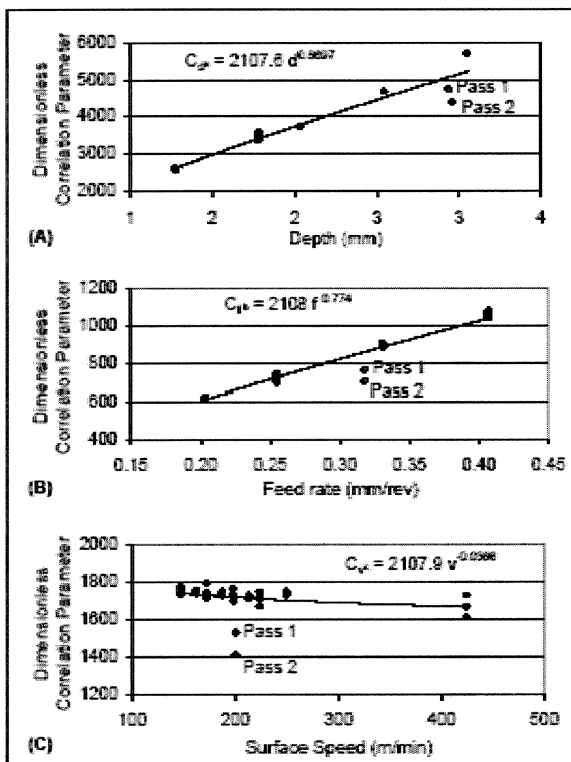


Figure 8: CNMG-432RN Model Plots for Depth (A), Feed (B), and Speed (C) with the Addition of Production Data Points (Circles)

Although the uncertainty of force measurements using the SLV method is higher than dynamometer measurements, monitoring cutting force through the SLV signal may be a more industrially-viable method than dynamometers due to the compromises in dynamic and static stiffness and limited resistance to coolant

introduced by dynamometers. Additionally, the SLV signal allows the cutting force to be monitored without sacrificing stiffness, thereby maintaining machine tool accuracy and part quality. Because the SLV method enables industry to collect process data which would otherwise be unknown, the SLV method remains valuable despite the increased measurement uncertainty when comparing the SLV method data to dynamometer data.

8. Acknowledgements

The authors would like to acknowledge the support and assistance of Alkan Donmez, Hans Soons, Mike McGlauffin and James Yost of the National Institute of Standards and Technology.

9. References

- 1) Merchant, E., 1998, Proceedings of the CIRP International Workshop on Modeling of Machining Operations, Atlanta, GA, USA.
- 2) Taylor, F. W., 1907, Trans. ASME 28:31.
- 3) Koenigsberger, F., 1964, Design Principals of Metal Cutting Machine Tools, Peragamon, Oxford.
- 4) Machining Data Handbook, 3rd Edition, 1980, Vol. 1 & 2, Metcut Reseach Associates Inc., Cincinnati, Ohio, USA.
- 5) Jurrrens, K., Soons, J., Ivester, R., 2003, "Smart Machining Research at the National Institute of Standards and Technology," DOE NNSA Small Lot Intelligent Manufacturing Workshop, Santa Fe, New Mexico, September 2-3 2003, proceedings number LA-14093, Los Alamos National Laboratory.
- 6) Ivester, R., Deshayes, L., McGlauffin, M., 2006, Determination of Parametric Uncertainties for Regression-Based Modeling of Turning Operations, NAMRC 34, Milwaukee, Wisconsin.
- 7) Ivester, R., Heigel, J., 2007, Smart Machining Systems: Robust Optimization and Adaptive Control Optimization For Turning Operations, Transactions of NAMRI 35, Ann Arbor, Michigan.
- 8) Marusich, T. D., Ortiz, M., 1995, "Modelling and Simulation of High-Speed Machining", *International Journal of Numerical Methods in Engineering*, 38/21:3675-3694.
- 9) Ivester, R., Whinton, E., Deshayes, L., 2005, Comparison of Measurements and Simulations for Machining of Aluminum, NAMRC 33, New York, New York.
- 10) Shaw, M. C., 1984, Metal Cutting Principles, Oxford Press, Oxford, UK.
- 11) Trent, 1991, Metal Cutting, Butterworth-Heinemann, Oxford.
- 12) Taylor, B. N., Kuyatt, C. C., 1994, Guidelines for Evaluating and Expressing the Uncertainty of NIST Measurement Results, NIST Technical Note 1297.

